Systematic error and correction of intensity-based I-PLIF for local pH and concentration measurements in unsteady boundary layers

Tom Lacassagne, Mahmoud El Hajem, Jean-Yves Champagne, Serge Simoëns

Systematic error and correction of intensity based I-PLIF for local pH and concentration measurements in unsteady boundary layers

Tom Lacassagne[1*], Mahmoud EL Hajem[2], Jean-Yves Champagne[2] and Serge Simoëns[2]

[1*]IMT Nord Europe, Institut Mines-Télécom, Univ. Lille, Centre for Energy and Environment, F-59000 Lille, France.
[2]Laboratoire de Mécanique des Fluides et d'Acoustique, UMR CNRS 5509, Univ. Lyon, INSA Lyon, Ecole Centrale de Lyon, Université Claude Bernard Lyon I, 20 avenue Albert Einstein, F-69621, Villeurbanne, France.

*Corresponding author(s). E-mail(s): tom.lacassagne@imt-nord-europe.fr;

Abstract

Planar Laser Induced Fluorescence methods, in particular in their Inhibited version (I-PLIF) are powerful tools to measure local scalar values in various types of flows. The most commonly used LIF methods are intensity-based: scalar value is extracted from fluoresced light intensity information. However such methods are prone to error when used in challenging configurations (multiphase flows, non-optically-thin systems, *etc*). In this short paper, the systematic error on concentration measurement in a dissolved gas boundary layer caused by scalar-dependency of the extinction coefficient is discussed, in the context of a non optically thin system with significant out-of-field absorption. Results of single color $\boldsymbol{I_{pH} - PLIF}$ measurements are compared to $\boldsymbol{I^r_{pH} - PLIF}$ (ratiometric) measurements for which the out-of-field absorption is intrinsically accounted for. An empirical correction based on first order concentration statistics derived from ratiometric measurements is proposed. It is used to demonstrate that the oversight of out-of-field absorption in intensity-based methods can lead to significant error on the scalar measurements inside the boundary layer.

Keywords: Planar Laser Induced Fluorescence, Calibration, Concentration, pH

1 Introduction

Achieving accurate, time resolved, and local measurement of scalar properties in complex liquid flows is a challenge in experimental fluid mechanics. Such measurements are highly desirable in heat and mass transfer studies, where they can be used to investigate mixing fundamentals (Bouche et al., 2013; Lacassagne et al., 2018). Planar Laser Induced Fluorescence (PLIF) methods are a powerful tool in that context. In their "classical" version, the local concentration of a fluorescent dye is related to its fluoresced light intensity triggered in a plane by a laser source, and the dye's dispersion and mixing is monitored by recording fluoresced light intensity using cameras (Papanicolaou and List, 1988). As an extension, the inhibited version of PLIF, I-PLIF, uses the scalar-dependency of well-mixed dye's fluorescence to "make visible" an intrinsic scalar quantity transported in the flow, and measure its local value, under some assumptions that are precisely discussed in the present work. Depending on the chosen dye, various flow scalars can be measured, such as temperature (Chaze et al., 2016; Mishra et al., 2019), pH (Asher and Pankow, 1986; Variano and Cowen, 2013; Valiorgue et al., 2013; Lacassagne et al., 2018; Kong et al., 2018) or dissolved gas concentration (Jimenez et al., 2014; Butler et al., 2016; Xu et al., 2020). PLIF methods yet face several limitations due to the fact that the local fluoresced light intensity also depends on the local laser excitation intensity mapping, which may not be homogeneous, especially in non optically thin systems. It may also be disturbed by unsteady phenomena such as reflections at gas liquid interfaces (Bouche et al., 2013; Butler et al., 2016), making all optical calibration steps performed in steady excitation condition non applicable. To account for such limitations, ratiometric methods have been developed (Coppeta and Rogers, 1998; Bouche et al., 2013; Chaze et al., 2016; Lacassagne et al., 2018; Kong et al., 2018). They no longer rely on fluoresced light intensity, but on the ratio of two fluoresced light intensities (colors, coming from one or multiple dyes) the value of which also depends on the scalar quantity to be measured. Ratiometric versions exist for "classical" (Bouche et al., 2013) or inhibited PLIF (Chaze et al., 2016; Lacassagne et al., 2018; Kong et al., 2018), and have been applied to mixing characterisation (Bouche et al., 2013), mass transfer measurements (Lacassagne et al., 2018; Kong et al., 2018), or temperature measurements (Chaze et al., 2016). In particular, pH sensitive techniques (Asher and Pankow, 1986; Valiorgue et al., 2013; Variano and Cowen, 2013; Lacassagne et al., 2018) are useful tools for fundamental and applied chemical engineering and process research in that they allow to quantify micro-mixing in presence of chemical reaction. They are nevertheless associated to an additional limitation inherent to the dyes used

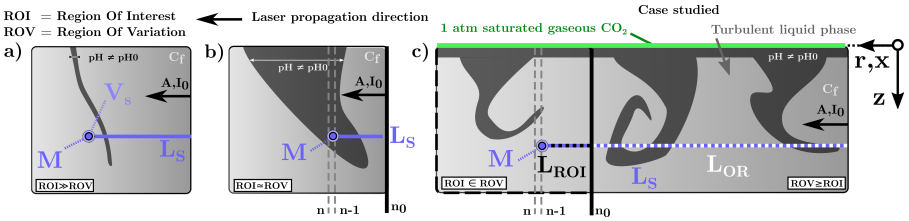

Figure 1 Configurations of high laser attenuation with scalar-dependent absorption coefficient a) easily correctable b) Correctable using a pixel-by-pixel method (Valiorgue et al., 2013), c) Non correctable with a single color method. The illustration is based on measurements reported in Lacassagne et al. (2022) used hereinafter.

(fluorescein sodium or others (Kong et al., 2018)): the scalar (pH) dependency of the absorption coefficient, which, in turn, affects the absorption of excitation intensity and makes the limitations of single color, intensity based PLIF even more critical. The constraints associated to scalar dependency of the absorption coefficient can be illustrated with figure 1, inspired and completed from Lacassagne et al. (2018).

In figure 1 a, the scalar's region of variation (ROV) is small compared to the region of homogeneous scalar, hence the absorption coefficient is only locally modified, and it can be assumed that the overall absorption as seen by a point M of the region of interest (ROI) "after" the scalar patch (in the laser propagation direction) is similar to what would have been without the scalar structure. Hence, a simple normalisation of the incident light intensity accounting for Beer-Lambert absorption is sufficient, and no further correction is required after calibration. In figure 1 b however, the scalar patch occupies a significant portion of the ROI, and thus the laser attenuation on its way through the ROI is significantly altered. This has an influence on the incident light effectively reaching the far side of the ROI. Progressive pixel-by-pixel calibration and processing as described in Valiorgue et al. (2013) are required to estimate the actual excitation intensity reaching each point of the ROI, which depends on the scalar structure encountered. Finally, figure 1 c corresponds to the critical case where most of the scalar structure encountered are outside of the ROI, in the so called outer region (OR). The laser path history on its way to the ROI is not known: it is not possible to account for out of field absorption (OFA) in the OR using elaborate pixel by pixel correction, and ratiometric methods are required. The above picture is a textbook example of challenges in unsteady scalar boundary layer measurements, where the size of the boundary layer in the liquid phase is often small compared to typical flow scales, forcing experimentalists to zoom the ROI well into the ROV, making optical access challenging, and measurement accuracy questionable (Valiorgue et al., 2013).

The objectives of this paper are twofold: firstly, understand and estimate the errors one makes when using single color PLIF in situations where the ratiometric method is *a priori* required; secondly, suggest a correction of single color concentration measurements in unsteady boundary layers based on the prior knowledge of the mean, steady, concentration profiles. For that purpose, a

data set presented in Lacassagne et al. (2022) is used. It corresponds to carbon dioxide dissolution and mass transfer at a flat horizontal gas liquid interface enhanced by bottom shear turbulence. pH sensitive laser induced fluorescence was applied in both its intensity-based ($I_{pH} - PLIF$) and ratiometric form ($I^r_{pH} - PLIF$), the pH decreasing with increasing dissolved gas concentration. Such measurements are well suited to the aims of this paper: they are targeting sub-millimetric scalar boundary layers in a flow of much larger scale, and thus focus on a ROI much smaller than the ROV and the OR, which is bound to be associated to significant, concentration dependent, and unsteady OFA.

All notations used throughout the present article (coordinates and parameters) are similar to those used in Lacassagne et al. (2022) (or Lacassagne et al. (2018)), unless stated otherwise. In what follows, the theoretical backgrounds of single color and ratiometric methods are recalled in section 2 (additional details available in Valiorgue et al. (2013) and Lacassagne et al. (2018), respectively). The experimental conditions reported in Lacassagne et al. (2022) are then briefly summarized in section 3. In section 4, the calibration strategies and data processing steps are first detailed, and the concentration results obtained with both methods are compared. The proposed correction is also assessed. As a conclusion, the origin of systematic error on single color measurement and its implications for the interpretation of literature measurements (including Lacassagne et al. (2018)) are discussed.

2 Theory

In Lacassagne et al. (2018), The recorded fluoresced light intensity coming from point M of the ROI for a given excitation wavelength λ_e is derived as

$$I_r(M) = I_0 A C_f \phi(M) \epsilon(\lambda_e, M) V_s . e^{-C_f \int_0^{L_s(M)} \epsilon(\lambda_e, r) dr} \tag{1}$$

where I_0 is the output laser intensity, A is a constant which depends on the optical set-up used to format the laser sheet, V_s is a small volume centred around M, $L_s(M)$ is the length crossed by a laser beam before reaching point M (see figure 1), C_f is the concentration of fluorescent dye in the fluid assumed identical at any point and ϕ and ϵ are the fluorescence quantum yield and extinction coefficient of the dye respectively. These last two quantities vary inside the fluid since they depend on local pH values. The above equation assumes that fluoresced light re-absorption on the way to the sensor is negligible (Lacassagne et al., 2018), and the present work is restricted to this assumption.

In single color methods a reference intensity field $I_{r,ref}$ measured at an homogeneous and known pH, pH_{ref}, is used to normalize recorded intensity fields, in order to account for non-homogeneity of I_0 and Beer-Lambert absorption. The non dimensional intensity at point M is then written

$$I^*(M) = \frac{I_r(M)}{I_{r,ref}(M)} = \frac{\phi(M).\epsilon(\lambda_e, M)}{\phi_{ref}.\epsilon_{ref}} . e^{-C_f \int_0^{L_s(M)} (\epsilon(\lambda_e, pH(r)) - \epsilon_{ref}) dr} \tag{2}$$

With $\phi_{ref} = \phi(pH_{ref})$ and $\epsilon_{ref} = \epsilon(\lambda_e, pH_{ref})$ the normalized quantum yield and extinction coefficients respectively. For the sake of simplicity, the λ_e dependency in the equations is dropped, as the laser source wavelength is most of the time known, unique and fixed in PLIF applications. The equations for the full fluoresced light spectrum are derived hereinafter, but similar equations can easily be written for specific fluorescence wavelengths λ or spectral band. One simply needs to replace ϕ by $S_\phi(\lambda)$ and if needed integrate the expressions over the chosen spectral band. It appears that in equation 2, laser reference intensity I_0 and the geometrical constant A have disappeared. However, the Beer-Lambert absorption term cannot *a priori* be cancelled out, since $\epsilon(\lambda_e, pH)$ generally differs from ϵ_{ref}. The expression of the received intensity thus still depends on laser absorption conditions.

In the ratiometric case however, bands of polychromatic fluoresced light are used instead of the full spectrum. The ratio R for fluoresced intensity integrated over two spectral bands (λ_1^{inf},λ_1^{sup}) and (λ_2^{inf},λ_2^{sup}) is

$$R(\lambda_1^{inf}, \lambda_1^{sup}, \lambda_2^{inf}, \lambda_2^{sup}, M) = \frac{\int_{\lambda_1^{inf}}^{\lambda_1^{sup}} S_\phi(\Lambda, M) d\Lambda}{\int_{\lambda_2^{inf}}^{\lambda_2^{sup}} S_\phi(\Lambda, M) d\Lambda} \tag{3}$$

with S_ϕ the "spectral" quantum yield of fluorescence. Demonstration of equation 3 can be found in Lacassagne et al. (2018), where it is shown that the ratio depends only on the pH (and thus on M), and this ratio is monotonous for well chosen spectral bands. In the present situation, L_s can be divided into two parts: L_{ROI} which corresponds to the laser path inside the ROI, accessible to measurement, and L_{OR} which is the path in the outer region. Assuming that laser beams are horizontal (weak laser sheet divergence) and the location of the ROI kept constant, the path crossed in the OR does not depend on M. The exponential terms in equation 2 can thus be separated and the equation becomes:

$$\begin{aligned} I^*(M) = & \frac{\phi(M).\epsilon(M)}{\phi_{ref}.\epsilon_{ref}} . e^{-C_f \int_0^{L_{OR}} (\epsilon(pH(r)) - \epsilon_{ref}) dr} \\ & . e^{-C_f \int_{L_{OR}}^{L_{OR}+L_{ROI}(M)} (\epsilon(pH(r)) - \epsilon_{ref}) dr} \end{aligned} \tag{4}$$

In conventional single color methods, both exponential terms of this equation are neglected as a first approach. For non-optically thin systems, it comes to assuming that the extinction coefficient stays close to its reference value during both calibration and the measurement steps. However in the present case, the variations of ϵ in the studied pH range are important, thus this simplification leads, as will be shown below, to substantial errors.

When $L_{OR} = 0$, or $L_{OR} << L_{ROI}$ with comparable absorption levels in the OR and ROI, the first exponential term of equation 4 approaches unity. This is the case where pixel-by-pixel calibration method as proposed by Valiorgue et al. (2013) can be applied. The principle is to no longer use the measured intensity but the normalized $(\phi\epsilon)^* = \frac{\phi\epsilon}{\phi_{ref}\epsilon_{ref}}$ as an indicator of pH. Contrary

to I^*, which depends on Beer-Lambert extinction of the laser intensity, the normalized ($\phi\epsilon$) quantity only varies according to the local pH.

In cases where $L_{OR} >> L_{ROI}$, the pixel-by-pixel calibration fails at accounting for absorption coefficient variation, as most of the laser absorption occurs outside of the ROI, beyond the experimental reach. On the other hand, one may assume that the absorption inside the ROI is negligible *versus* that in the OR. This applies for example for experiments where L_{OR} is of the order of 10 cm or 1 m, and L_{ROI} of the order of 1 cm, with similar phenomena occurring in OR and ROI regions. The first exponential term of equations 4 is no longer close to unity, but the second exponential term is, and the correction method proposed below applies in that case. Indeed, in order to account for OR variations of extinction coefficient, one needs information on the local value of pH in the OR, which is precisely the quantity that is measured in the ROI. A way of getting around this problem is to rewrite the exponential term of equation 2 as

$$e^{C_f \int_0^{L_{OR}} (\epsilon(r) - \epsilon_{ref}) dr} = e^{C_f L_{OR} (\overline{\epsilon} - \epsilon_{ref})} \tag{5}$$

where $\overline{\epsilon}$ is the average extinction coefficient along L_{OR}. Its value depends on the concentration statistics. In the case depicted in figure 1 (as in Lacassagne et al. (2022)), the beams propagation and thus the r direction is horizontal, noted $r \equiv x$, and scalar quantities vary along the vertical direction z. As a first order approximation, one may write that

$$\overline{\epsilon}(z,t) = f\left(\overline{C}(z,t)\right) \tag{6}$$

where C is the pH dependent scalar quantity, in that case dissolved carbon dioxide concentration, which itself influences the local ϵ values. The over-bar symbol denotes a width averaged profile of the extinction coefficient (along the laser path-line), leaving only a depth (z) and time (t) dependency. All that is needed is then an information on the (instantaneous) mean concentration profile in the boundary layer, as ϵ directly depends on C. In what follows, instantaneous concentration profiles obtained from ratiometric measurements will be used to try and correct single color measurements of the same experiment.

3 Experiments

The experiments reported in Lacassagne et al. (2022) consisted in pure gaseous carbon dioxide dissolving in a liquid phase from a flat horizontal interface, under the action of turbulence in the liquid phase (figure 1 c, schematic representation, not to scale). The ROI was located at the center of a large tank, and the ROV was wide as the surface of exchanges. An empirical correlation between dissolved gas concentration and pH was $C = Ae^{-BpH}$ with A=1.55×10^{11} mg/L and $B = 4.63$ (from Lacassagne (2018); Lacassagne et al. (2022)).

$I_{pH} - PLIF$ (using the full fluorescence spectrum) and $I^r_{pH} - PLIF$, with the same spectral bands as used in Lacassagne et al. (2018) were used to collect fluoresced light intensity fields. The fluorescent dye was fluorescein dissodium salt at a concentration of $C_f = 5.10^{-7}$ M. Fluorescence was triggered by a Stabilite 2017 Argon-Ion Continuous Wave Laser (CWL) and recorded by a Lavision 2560 by 2160 sCMOS sensor equipped with a 105 mm focal length Macro lens. For $I_{pH} - PLIF$ measurements, the lens was only equipped with a long-pass filter to suppress the fluorescence excitation wavelength. For $I^r_{pH} - PLIF$ measurements, an image doubler was added in front of the lens. One "eye" of the doubler was equipped with a 515 nm bandpass filter (band 1: $\lambda_1^{inf} = 510$ nm, $\lambda_1^{sup} = 520$ nm), and the other with a 560 nm cut-off long-pass filter (band 2: $\lambda_2^{inf} = 560$ nm, $\lambda_2^{sup} \longrightarrow +\infty$). The shutter time was $\mathrm{d}t_f = 10$ ms.

Due to the central location and small size of the ROI with respect to the tank in the experiments, PLIF measurements were performed in the situation described in figure 1 c: $L_{OR} = 12$ cm and $L_{ROI} = 2$ cm: the system cannot be considered optically thin, and laser excitation intensity received by a given point of the ROI was conditioned by Beer-Lambert absorption. This absorption depended on dissolved gas structures encountered by the laser on its path, inside and outside of the ROI, because the absorption coefficient on fluorescein sodium depends itself on the pH, which in turn depends on the dissolved gas concentration to be measured. Concentrations measured by the two-color method and their statistics will be used as reference values, keeping in mind that $I^r_{pH} - PLIF$ is also subject to measurement errors as discussed extensively in Lacassagne et al. (2018).

Hereinafter, two single color procedures are applied. Firstly the Standard procedure **S** assumes that $e^{C_f L_s(\epsilon(pH) - \epsilon_{ref})}$=1 during both the calibration and measurement steps. It is the fastest single color method in terms of processing time, since it only requires the normalization of calibration and measurement images by a unique reference image recorded at an homogeneous and known pH. It is also the most frequently encountered in the literature. It is however expected to lead to significant errors, since the variations of extinction coefficient are neglected. Single-color PLIF is applied using that of the two available fluorescence signals with the best signal-to-noise ratio. Similar results have been obtained using the lower intensity spectral band, with yet a higher noise level. Secondly, the Standard procedure accounting for absorption in the outer region, labelled **Sa**, consists in applying equations 4 and 5, neglecting absorption inside the ROI, and using the mean concentration profile obtained from ratiometric measurement as an input data (equation 6). In doing so, one assumes that scalar fields in the ROI and OR are comparable, and that the ROI is large enough with respect to the scalar structure so that it provides first order concentration statistics that are representative of the whole ROV and thus of the OR. In other words, the hypothesis is that the concentration field is statistically homogeneous along the beam penetration direction, and in so, the mean concentration values have to be the same along this direction. These

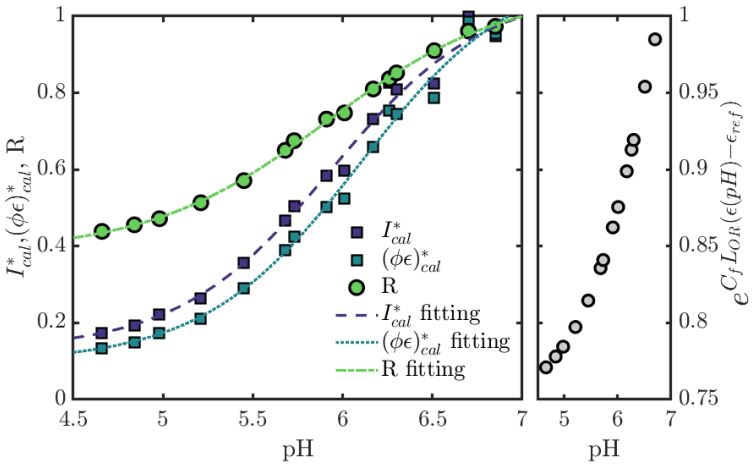

Figure 2 Calibration curves for single color methods S and Sa, and for the ratiometric method R. Markers are points measured from calibration images for respectively I^*_{cal}, $(\phi\epsilon)^*_{cal}$ and R. Dashed and dotted lines are hyperbolic tangent fittings. The exponential corrective factor $e^{C_f L_{OR}(\epsilon(pH)-\epsilon_{ref})}$ is plotted versus pH in subfigure b.

two procedures are tested on one single arbitrarily chosen instantaneous field (t=200 s), and compared to the ratiometric procedure **R**, also performed on the same instantaneous data. A similar analysis has been performed for the S and Sa procedures on other instantaneous fields and led to the same conclusions. Calibration images were recorded at several homogeneous pH values (see figure 2). The same processing (S, Sa or R) was applied to calibration images to derive the intensity or ratio *versus* pH calibration relationships.

4 Results

Figure 2 shows calibration curves for the S, Sa and R methods. Markers are measured points and lines are hyperbolic tangent fittings. It appears that the $(\phi\epsilon)^*_{cal}$ relative values are lower than I^*_{cal} values, especially at low pH. Indeed, taking $\epsilon_{ref} = \epsilon(7)$, the difference $\epsilon(pH) - \epsilon_{ref}$ is negative since the absorption coefficient decreases with decreasing pH (see figure 2, Klonis and Sawyer (1996)). The OR exponential correction term computed from equation 4 here ranges from about 0.75 to unity at pH=7 (figure 2 b).

Absorption in the outer region is predicted from ratiometric concentration measurements. The mean concentration profile $\overline{C}(z,)$ obtained is turned into $\overline{pH}(z)$ using the previously established pH-C calibration. $\overline{pH}(z)$ is translated into $\overline{\epsilon}(z)$ thanks to hyperbolic tangent fitting of the literature data for epsilon (Lacassagne et al., 2018), and the exponential factor $e^{C_f L_{OR}(\overline{\epsilon}(z)-\epsilon_{ref})}$ can be computed as a function of z.

All these profiles are shown respectively in figure 3 a), b), c) and d), in log scale z axis and log scale concentration values for sub-figure a). Dissolved

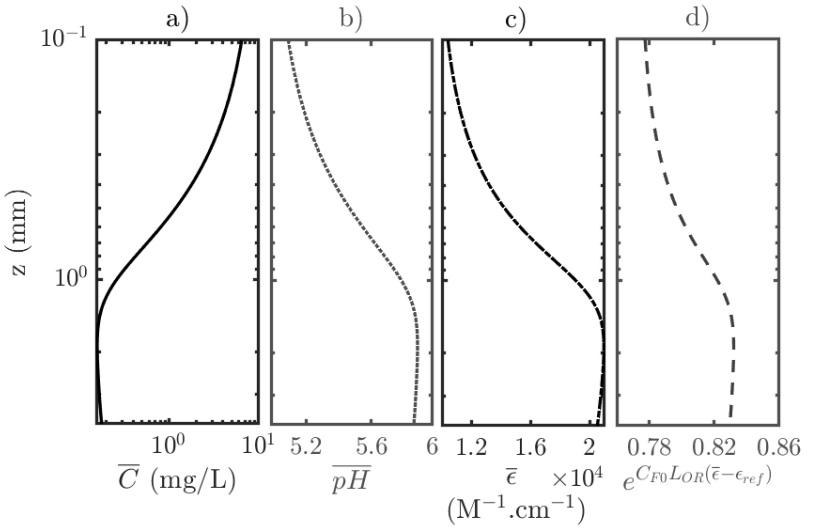

Figure 3 Correction of the outer region absorption based on ratiometric measurement of $\overline{C}(z,t)$, with t=200 s. a) is $\overline{C}$ profile in log-log scale. b)c)d) are profiles for $\overline{pH}$, $\overline{\epsilon}$ and $e^{C_f L_{OR}(\overline{\epsilon}-\epsilon_{ref})}$ respectively, z in log scale.

gas concentration in the OR leads to correction factors between 0.75 and 0.85, even at the greatest depths where concentration is minimum. In other words, accounting for OFA leads to downgrade by up to 25% the measured fluoresced light intensity values. It should yet be noted that this correction factor has to be considered together with the one on calibration curves: during the calibration process, pH is homogeneous in the tank so no such profile exists, however, the OR absorption for the lowest calibrated pH values is smaller than the OR absorption for the higher ones. This explains the difference in the I^*_{cal} and $(\phi\epsilon)^*_{cal}$ curves in figure 2.

Looking now at instantaneous in-flow measurements, the concentration and pH fields in figure 4 are visually very similar. This shows that scalar fields are qualitatively well captured by all methods. However, it appears that the S method underestimates concentration levels, especially at high concentrations. Correction of outer region absorption makes Sa fields more similar to R fields even if some scalar structures still seem of lower concentration in the Sa picture than in the R one. pH fields from single color methods never display values higher than 6.5 while the reference pH=7 is reached at some regions of the field obtained from ratiometric measurement. This however does not impact much concentration levels since pH between 6.5 and 7 correspond to low concentration values (lower than 10^{-1} mg/L here). pH fields S and Sa are visually difficult to compare: variations are of about 0.1 to 0.2 pH units. Yet because of the exponential link between pH and concentration this leads to important differences in terms of local concentration values.

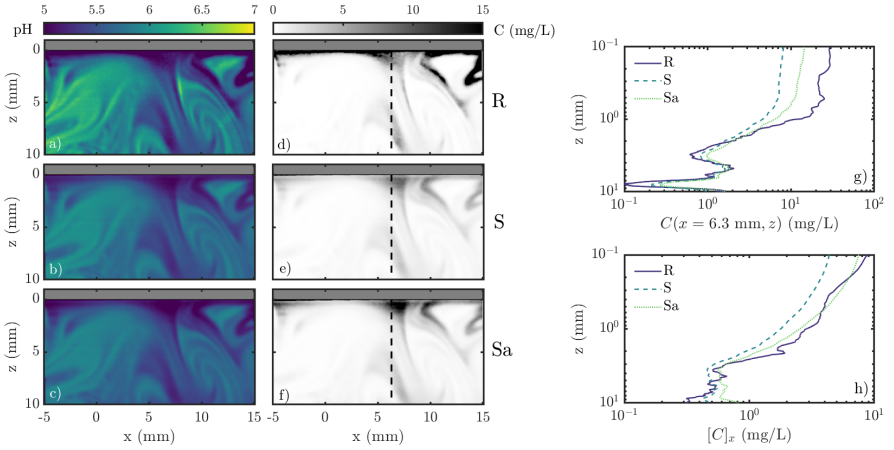

Figure 4 Comparison of pH (a,b,c) and concentration (d,e,f) fields obtained by R (a,d), S (b,e) and Sa (c,f) methods, and comparison of g) local (x=6.3 mm, vertical dashed lines) and h) width averaged concentration profiles along depth, obtained by all three methods, in log-log scale.

The final comparison is made by extracting concentration profiles along depth at a given x value, here x=6.3 mm (figure 4 g)), and by computing the width averaged concentration profile over the ROI (figure 4 h)). Local profiles at x=6.3 mm confirm that single color measurements yield lower concentration values than the ratiometric one. Correction of the OR absorption allows to increase the measured concentration values but not exactly up to those measured by the R method. However when averaging over the ROI's width, it appears than the $[C]_x$ values obtained by the Sa method are similar to those obtained by the R method. Last but not least, the shape of the concentration profiles are unaffected by the method used to estimate them. Concentration values vary, but not their evolution with depth. It is of great interest since it implies that single color measurements can still be used for qualitative comparison of concentration structures and profiles with ratiometric measurements.

5 Conclusions

The use of single color PLIF without any specific correction in a condition where absorption occurs outside of the ROI globally leads to slightly over estimate pH values and ultimately to a significant under estimation of concentration values. This can be explained in the following way. During calibration, images are recorded in conditions that are somehow different from the measurement conditions: with a pH homogeneous over the full laser path in the fluid. During the experiment, the laser beam at a given depth z sees an average absorption value $\bar{\epsilon}$ defined by the mean concentration profile, hence by the measured phenomena. Because of the presence of the boundary layer and of high concentration scalar patches (figure 4), this average absorption is always

smaller than the reference one, if the reference is chosen constant at higher pH, and excitation beams reach the ROI at a higher intensity level than expected from the intensity calibration images I^*_{cal}. Neglecting extinction coefficient variations in the OR thus comes to interpret higher recorded intensity levels as being caused by higher local pHs (and lower dissolved gas concentrations, here), whereas they are in fact due to an increased local excitation intensity.

A notable result is yet that this under-estimation does not affect the spatial distribution of concentration structures or profiles along depth. It only changes the magnitude of the concentration. To that extend, while the accuracy of single color methods for quantitative measurements can be questioned, they can still be used for analysing of the shape of scalar structures, and of qualitative evolution of scalar and mass flux statistics in space.

References

Asher, W.E. and J.F. Pankow. 1986, November. The interaction of mechanically generated turbulence and interfacial films with a liquid phase controlled gas/liquid transport process. *Tellus B 38B*(5): 305–318. https://doi.org/10.1111/j.1600-0889.1986.tb00256.x .

Bouche, E., S. Cazin, V. Roig, and F. Risso. 2013, June. Mixing in a swarm of bubbles rising in a confined cell measured by mean of PLIF with two different dyes. *Experiments in Fluids 54*(6): 1552. https://doi.org/10.1007/s00348-013-1552-0 .

Butler, C., E. Cid, and A.M. Billet. 2016, November. Modelling of mass transfer in Taylor flow: Investigation with the PLIF-I technique. *Chemical Engineering Research and Design 115*(Part B): 292–302. https://doi.org/10.1016/j.cherd.2016.09.001 .

Chaze, W., O. Caballina, G. Castanet, and F. Lemoine. 2016, April. The saturation of the fluorescence and its consequences for laser-induced fluorescence thermometry in liquid flows. *Experiments in Fluids 57*(4): 58. https://doi.org/10.1007/s00348-016-2142-8 .

Coppeta, J. and C. Rogers. 1998. Dual emission laser induced fluorescence for direct planar scalar behavior measurements. *Experiments in Fluids 25*(1): 1–15. https://doi.org/10.1007/s003480050202 .

Jimenez, M., N. Dietrich, J.R. Grace, and G. Hébrard. 2014, July. Oxygen mass transfer and hydrodynamic behaviour in wastewater: Determination of local impact of surfactants by visualization techniques. *Water Research* 58: 111–121. https://doi.org/10.1016/j.watres.2014.03.065 .

Klonis, N. and W.H. Sawyer. 1996. Spectral properties of the prototropic forms of fluorescein in aqueous solution. *Journal of Fluorescence 6*(3): 147–157.

https://doi.org/10.1007/BF00732054 .

Kong, G., K.A. Buist, E.A.J.F. Peters, and J.A.M. Kuipers. 2018, May. Dual emission LIF technique for pH and concentration field measurement around a rising bubble. *Experimental Thermal and Fluid Science* 93: 186–194. https://doi.org/10.1016/j.expthermflusci.2017.12.032 .

Lacassagne, T. 2018. *Oscillating grid turbulence and its influence on gas liquid mass transfer and mixing in non-Newtonian media.* PhD Thesis, University of Lyon, INSA Lyon.

Lacassagne, T., M. EL Hajem, J.Y. Champagne, and S. Simoëns. 2022. Turbulent mass transfer near gas-liquid interfaces in water and shear-thinning dilute polymer solution. *International Journal of Heat and Mass Transfer* 194: 122975. https://doi.org/10.1016/j.ijheatmasstransfer.2022.122975 .

Lacassagne, T., S. Simoëns, M.E. Hajem, and J.Y. Champagne. 2018, January. Ratiometric, single-dye, pH-sensitive inhibited laser-induced fluorescence for the characterization of mixing and mass transfer. *Experiments in Fluids 59*(1): 21. https://doi.org/10.1007/s00348-017-2475-y .

Mishra, Y.N., A. Yoganantham, M. Koegl, and L. Zigan. 2019, December. Investigation of Five Organic Dyes in Ethanol and Butanol for Two-Color Laser-Induced Fluorescence Ratio Thermometry. *Optics 1*(1): 1–17. https://doi.org/10.3390/opt1010001 .

Papanicolaou, P.N. and E.J. List. 1988, October. Investigations of round vertical turbulent buoyant jets. *Journal of Fluid Mechanics* 195: 341–391. https://doi.org/10.1017/S0022112088002447 .

Valiorgue, P., N. Souzy, M. EL Hajem, H.B. Hadid, and S. Simoëns. 2013, April. Concentration measurement in the wake of a free rising bubble using planar laser-induced fluorescence (PLIF) with a calibration taking into account fluorescence extinction variations. *Experiments in Fluids 54*(4): 1–10. https://doi.org/10.1007/s00348-013-1501-y .

Variano, E.A. and E.A. Cowen. 2013, September. Turbulent transport of a high-Schmidt-number scalar near an air–water interface. *Journal of Fluid Mechanics* 731: 259–287. https://doi.org/10.1017/jfm.2013.273 .

Xu, F., G. Hébrard, and N. Dietrich. 2020, April. Comparison of three different techniques for gas-liquid mass transfer visualization. *International Journal of Heat and Mass Transfer* 150: 119261. https://doi.org/10.1016/j.ijheatmasstransfer.2019.119261 .